INL/EXT-06-11760

Experimental Modeling of VHTR Plenum Flows During Normal Operation and Pressurized Conduction Cooldown

Glenn E. McCreery
Keith G. Condie

September 2006

The INL is a U.S. Department of Energy National Laboratory
operated by Battelle Energy Alliance

INL/EXT-06-11760

Experimental Modeling of VHTR Plenum Flows During Normal Operation and Pressurized Conduction Cooldown

Glenn E. McCreery
Keith G. Condie

September 2006

Idaho National Laboratory
Idaho Falls, Idaho 83415

Prepared for the
U.S. Department of Energy
Office of Nuclear Energy
Under DOE Idaho Operations Office
Contract DE-AC07-05ID14517

Experimental Modeling of VHTR Plenum Flows during Normal Operation and Pressurized Conduction Cooldown

Glenn E. McCreery and Keith G. Condie

The Very High Temperature Reactor (VHTR) is the leading candidate for the Next Generation Nuclear Power (NGNP) Project in the U.S. which has the goal of demonstrating the production of emissions free electricity and hydrogen by 2015 (MacDonald et al., 2003). VHTR vessel thermal-hydraulic phenomena that are of importance during normal, reduced power, and accident operation were identified by McEligot and McCreery, 2004, and are indicated in Figure 1. The present document addresses experimental modeling of flow and thermal mixing phenomena of importance during normal or reduced power operation and during a loss of forced reactor cooling (pressurized conduction cooldown) scenario. The objectives of the experiments are, 1), provide benchmark data for assessment and improvement of codes proposed for NGNP designs and safety studies, and, 2), obtain a better understanding of related phenomena, behavior and needs.

Physical models of VHTR vessel upper and lower plenums which use various working fluids to scale phenomena of interest are presented and the recommended water-flow models are described in more detail. The models may be used to both simulate natural convection conditions during pressurized conduction cooldown and turbulent lower plenum flow during normal or reduced power operation. Benchmark data that will be provided by the experiments are:

Lower plenum temperature distribution during turbulent forced convection (the “hot streaking” or “thermal striping” problem).

Lower plenum velocity and temperature fields during the decay heat period of a pressurized conduction-cooldown (laminar natural circulation flows).

Upper plenum velocity and temperature fields during a pressurized conduction-cooldown (laminar natural circulation flows).

Background

A number of previously conducted analyses and experiments are relevant to the present study. A few of these are described. Thermal fluctuations in the lower plenum of a high-temperature gas-cooled reactor of the French CEA design were investigated analytically by Tauveron, 2002. The calculations illustrate the complexity of the flow and the thermal

loading imposed on internal structures. Scaled experiments were conducted at the INL which investigated off-normal and accident conditions in the upper plenum of a Savannah River Site nuclear reactor (McCreery et al., 1991). The experiments illustrate the complexity of flow and mixing in a plenum containing a large number of cylindrical and other shaped components. Many studies of cross-flow in tube bundles, single and multiple jets mixing in confined spaces are reported in the literature and the references were compiled by King, 2004. Experiments which modeled natural circulation during PWR severe accidents were conducted at Westinghouse Electric Corporation (Westinghouse Electric Corporation, 1990) using sulfur hexafluoride (SFl6) in a 1/7 geometrically scaled model facility. Flow in the reactor vessel connected to two loops containing model steam generators were simulated in the electrically heated facility.

Several previously conducted experiments investigated hot-streaking in specific gas-cooled reactor core outlets which, although the lower plenum geometries are different from the VHTR, have some relevance to the present study. Experiments were conducted to characterize thermal mixing and hot streaking in the lower plenum (core bottom structure, CBS) of the gas-cooled high temperature engineering test reactor (HTTR) developed by the Japan Atomic Energy Institute (JAERI). Initial experiments (Inagaki, et al., 1990) were carried out using a one-seventh scale model of the CBS including a plenum and outlet hot gas duct with water as the test fluid. Hot and cold water were injected into the model and the temperature distributions of the mixed water were measured. Follow-on experiments were conducted using a full-scale model of the vessel (Inagaki, et al., 1991), including the CBS, in the heated helium engineering demonstration test loop (HENDL). It was determined that, with the inclusion of a mixing promoter, that mixing was sufficient to prevent significant thermal striping (greater than a 15 ^{o}C variation according to their definition). Core outlet temperature mixing in the outlet plenum (hot gas header) of the helium cooled modular high temperature reactor (HTR) developed by Interatom and Siemens was investigated in a 1:2.9 scaled plastic model using heated air flow (Damm and Wehrlein, 1990). Colder gas leakages into the plenum were also simulated in the model. The favorably high mixing rate allowed the plenum design to be simplified by changing a complex network of mixing channels into simple straight channels and by reducing the volume of the plenum. Thermal mixing in the lower plenum (hot gas chamber) of the high temperature gas-cooled pebble-bed reactor test module (HTR-10) located at Tsinghua University, China, was investigated in a 1:1.5 scale model using heated air flow (Yao, et al., 2002). Gas mixing takes place in cavities between eight supporting ribs and then flows out radially into a circumferential channel and then into a horizontal outlet pipe. Four different flow mixing arrangements were investigated. All arrangements except an empty plenum provided acceptable mixing. Although these reactors are much smaller than the proposed VHTR and none of the lower plenum geometries investigated have much similarity to the VHTR lower plenum, the experimental methods and results help give confidence to the experimental modeling methods proposed in this document.

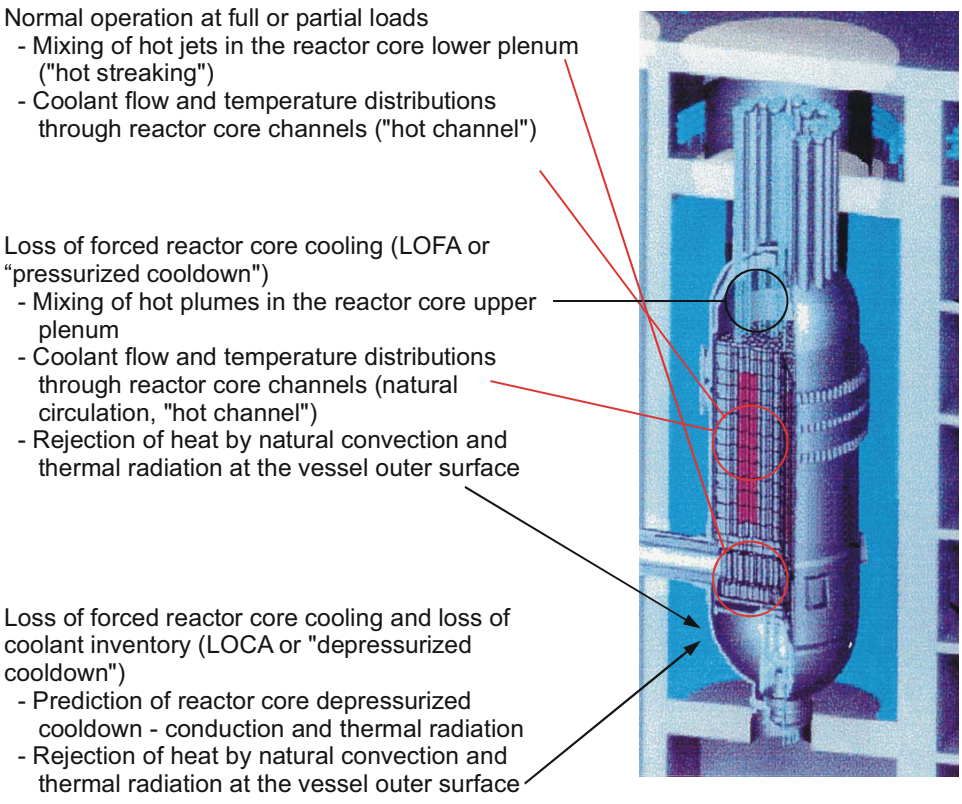

Figure 1. Important VHTR thermal-hydraulic phenomena.

Model Conceptual Design and Scaling Approach

Code predictions of VHTR core flow during a pressurized-conduction-cooldown scenario (Bayless, 2006) indicate that channel-to-channel flow is important with upflow occurring in the more central channels and downflow occurring in the peripheral channels. An experimental apparatus capable of simulating three-dimensional (laminar) natural circulation flows in the upper and lower plenums can either generate the channel flows by heating the fluid in simulated core channels or provide the simulated channel flows from an external source; blowers in the case of gas flow or pumps in the case of water flow. In addition, the apparatus design must be capable of delivering higher turbulent flow to the lower plenum to simulate thermal mixing during normal operation forced circulation in the lower plenum (the “thermal striping” or “hot streaking” problem). A suitable apparatus needs to be geometrically scaled to the prototype so that velocity ratios, an important scaling criterion for mixing, are preserved. Employing the one-half symmetry of the prototype lower plenum permits improved instrumentation and visibility and reduced total flow rate (by ½) as compared with a full cylindrical model. A one-half symmetric lower plenum apparatus is shown schematically in Figure 2. The upper

plenum may be scaled to either complete, one-half, or one-quarter of the prototype. A one-quarter symmetric upper plenum model is shown in Figure 3. The one-quarter symmetric upper plenum model is preferred because of simplicity and because for a water-filled model a one-quarter symmetric upper plenum (as shown schematically in Figure 3) permits laser light sheets to illuminate the plenum for side-views without the added distortions of a water-filled rectangular box surrounding the plenum (top views of the plenum will still require a water filled box). A water-filled rectangular box is required to eliminate distortion caused by non index-matching surfaces (water, plastic, and air) by providing plane-surface windows.

The several models considered in this study are all geometrically (linearly) scaled to the prototype except for the core channels, which are too small, 7.9 mm in diameter, and too numerous, on the order of 11,000, to geometrically scale. The flows modeled are assumed to be quasi steady-state which computer code calculations indicate is a reasonable assumption for the normal power and decay heat conditions considered. Fast transients, such as LOCA's, are not considered. All models are assumed to have the same geometric scaling ratio, S, of 1/6.55, which is the same scaling ratio as employed for the Matched-Index of Refraction (MIR) lower plenum model (McElroy et al., 2006). This ratio is chosen for practical reasons including the availability of materials, optical access, and pumping requirements, as well as the ease of implementing experimental methods developed for the MIR experiments and comparing the present experimental results with MIR experimental data.

Several circulation methods and fluids were investigated for implementation in the model. Results of scaling calculations and practical considerations are summarized in Table 1. The method most conceptually similar to the prototype would be to employ electrically heated tubes with atmospheric pressure nitrogen or another gas, such as sulfur hexafluoride, to induce natural convection in the core. An external heat exchanger would be necessary to remove heat generated in the simulated core. An external blower would be necessary to drive forced convection flow. This concept is shown in Figure 4. Rather than using heated gas flow, buoyancy forces might be simulated by injecting a heavier gas, such as argon or sulfur hexafluoride, into channels which represent lower heat transfer channels in the prototype and a lighter gas into channels which represent higher heat transfer. The gas mixture flowing through the upper plenum would be removed as it enters the outer, simulated low heat transfer, channels and replaced with the heavier gas. Of the two gas flow methods, the scaling consideration of providing closer Reynolds numbers at matching Richardson numbers to prototypical values and construction and operation and other practicality considerations favor the heavy-gas injection method. However, the disposal of or recapturing and separating large volumes of a heavy gas is a major difficulty with the method.

Rather than using gas flow, water flow may be used to simulate forced and natural circulation flow in the prototype. Buoyancy forces within the plenums can be simulated by either heating the water or by adding a dissolved substance, such as salt, to increase the water density in channels representing lower heat transfer channels in the prototype. However, concerns about the disposal of large quantities of salt water make this latter

approach impractical. The heated water flow method provides the closest match of Reynolds numbers at prototypical Richardson numbers, especially for lower plenum flow. Comparing gas flow and water flow methods; the venting of large quantities of gas and increased measurement difficulties compared to water flow, favor the heated water flow method. Heated water flow is therefore the preferred choice. Although natural circulation is to be simulated, the power requirements of heating water in a simulated core to drive the flow are excessive. Therefore, flow will be delivered by pumps from two reservoirs which contain heated water in one reservoir and unheated water in the other (Figure 5). Reservoir sizes will be chosen to provide sufficient time to collect data once flow and temperatures are at steady-state operating conditions. Approximately five minutes is sufficient time (including start-up) to obtain PIV and thermocouple measurements. Reservoir sizes will therefore need to be approximately 1,000 gallons in order to sustain the 200 GPM needed for maximum flow (Table 1). Flow rates and temperature boundary conditions will be provided by ATHENA/RELAP5-3D calculations. The 134 channels are subdivided into nine heat transfer regions which correspond to the nine core regions used in the VHTR ATHENA/RELAP5-3D model of Bayless, 2006 (Figure 6).

Relevant Scaling Equations

The general approach to scaling experiments that simulate natural circulation in the prototype reactor plenums in the water-flow facility is to match both Richardson number, the ratio of buoyant to inertial forces, and Reynolds number, the ratio of inertial to viscous forces. The approach to scaling experiments that simulate turbulent forced circulation in the lower plenum during normal operation is to insure that flow is fully turbulent in each component. This is insured if Reynolds number for flow in the smallest nozzle entering the lower plenum is greater than approximately 4,000. Reynolds numbers will necessarily be lower than in the prototype. For fully turbulent flow, buoyant forces will be much lower than inertial forces and Richardson number scaling may therefore be ignored. Instead, a small but measurable temperature range (e.g. 10 ^{o}C) will be employed to quantify mixing.

The primary forces involved in scaling convective flow involving a temperature gradient are inertia, buoyancy, and viscous dissipation (Turner, 1973). Temperature variations within a convective flow give rise to variations in properties of the fluid. The mass, momentum and energy equations describing the flow are commonly used in a form known as the Boussinesq approximation, where variations of fluid properties other than density as it gives rise to gravitational force are ignored. The Boussinesq approximation for density (ρ) change is,

$$\rho = \rho_0 + \Delta\rho$$

With this approximation, the Navier-Stokes equation becomes (Triton, 1977),

$$\frac{D\overline{V}}{Dt} = -\frac{\nabla P}{\rho} + \nu\nabla^2\overline{V} + \frac{\Delta\rho}{\rho}\overline{g}$$

Where, $\overline{V}$ is (vector) velocity, t is time, P is pressure, ν is kinematic viscosity, and $\overline{g}$ is the gravitational acceleration.

For a density variation due to temperature, the dependence of ρ on T may be expressed as,

$$\Delta\rho = -\alpha\rho_0\Delta T$$

Where, α is the thermal expansion coefficient, = 1/T for a perfect gas.

The ratio of buoyant to inertia forces is the Richardson number, which may be expressed in terms of either a density difference or a temperature difference, and a relevant length, D, as,

$$Ri = \frac{g(\ (\rho_0 - \rho\ )/\rho_0)D}{V^2} = \frac{g\alpha\Delta TD}{V^2} = \frac{g(\Delta T/T)D}{V^2}$$

The ratio of Richardson numbers of the model (m) and prototype (p) is then,

$$\frac{Ri_m}{Ri_p} = \frac{\left(\frac{\Delta\rho}{\rho}\right)_m}{\left(\frac{\Delta\rho}{\rho}\right)_p}\frac{V_p^2}{V_m^2}\frac{D_m}{D_p}$$

The Reynolds number, the ratio of inertial to viscous forces, is,

$$\mathrm{Re} = VD/\nu$$

If, for the natural circulation experiments, Richardson number is matched in the model and prototype, then the Reynolds number ratio for model and prototype may be expressed as,

$$\frac{\mathrm{Re}_m}{\mathrm{Re}_p} = \frac{V_m D_m \nu_p}{V_p D_p \nu_m} = \left[\frac{\left(\frac{\Delta\rho}{\rho}\right)_m}{\left(\frac{\Delta\rho}{\rho}\right)_p}\right]^{1/2}\left[\frac{D_m}{D_p}\right]^{3/2}\frac{\nu_p}{\nu_m}$$

Calculations using the above equations indicate that, for gas flow, model Reynolds number will be a fraction of that of the prototype for realistically achievable temperatures and density ratios in a model facility operated at close to atmospheric pressure (see Table 1). However, for water flow, the equations indicates that both Richardson and Reynolds numbers of the lower plenum model may be approximately matched to the prototype for reasonable cold and hot water temperatures (approximately 20 C cold and 46 C maximum hot respectively, as shown in Figure 7). This matching is possible in a scale model primarily because of the considerably higher kinematic viscosity of helium compared with water. It is more important to match Reynolds number in laminar flow natural circulation experiments than in turbulent flow experiments, since quantities such as mixing, drag coefficients and eddy dimensions are a much stronger function of Reynolds number in laminar flow.

The above equations apply to both the upper and lower plenums. However, the Reynolds numbers for the channels connecting to the upper plenum will be distorted because the large number of channels in the prototype (approximately 11,000 total, or 2,750 connecting to one-quarter of the plenum) will necessarily be modeled using fewer channels in the model. Reducing the number of channels and locations to the corresponding distribution in the lower plenum (67 channels for a ¼ representation) will permit the use of the same plumbing system for either experiment. The connection of core channels to lower plenum nozzles (and therefore the correspondence of core channels in the prototype with the choice of channels connected to the upper plenum in the model) is shown in figure 8. Because the temperature differences entering the upper plenum are greater than those entering the lower plenum (Figure 7), and because the maximum temperature difference between channels in the model is limited to approximately 60 ^{o}C or less, Reynolds numbers in the model upper plenum will be further distorted at matching Richardson numbers.

If Richardson numbers based on channel-to-channel temperature differences and on plenum diameter and internal components other than the channels are matched, and if the sum total of channel flow areas is scaled as $1/S^2$, which insures that velocity ratios of the channels and upper plenum components are maintained, then channel Reynolds number will be high by approximately a factor of three (the flow will still be laminar) and Reynolds numbers for internal components will be low by approximately a factor of three. These results assume that the maximum water temperature is limited to 46 ^{o}C, the same as for the lower plenum model.

Another variation on the scaling approach for the upper plenum is to match Richardson numbers based on channel dimensions and temperatures, which will then cause distortions in Ri and Re for other components. A series of experiments will need to be conducted over ranges of Richardson and Reynolds numbers to characterize these distortions.

Other Scaling Considerations

Although the majority of phenomena of interest are properly scaled with Richardson and Reynolds numbers, several effects, which include wall heat transfer, jet inlet conditions, jet entrainment and eddy shedding require further consideration. These include the following:

The heat transfer effects of hot or cold surfaces are not modeled. However, calculations by Bayless, 2004, indicate that the plenum walls during a conduction-cooldown scenario may be considered to be adiabatic. Since internal components have less mass than the walls, they may also be considered adiabatic.

Jet flow, as it enters the lower plenum, is influenced by the jet boundary conditions. Turbulent jet flow downstream of the entry is strongly influenced by entry geometry, according to Nobes and Nathan, 2001. Entry nozzle geometry and upstream development length/diameter therefore need to be similar in the model and prototype. For natural circulation conditions, the jets need to be well-developed (with a parabolic velocity profile).

Entrainment of ambient fluid into free jets issuing from nozzles is investigated in Appendix 1. It is concluded that jet entrainment and jet-to-jet interaction in a geometrically scaled facility should be scaled properly and be approximately independent of Reynolds number. However, since the channels entering the upper plenum are not geometrically scaled to the prototype, there will be distortions in entrainment and jet interactions. Because of this, the jets will merge at greater scaled distance from the channel entrances to the upper plenum than in the prototype. The distance for jets to merge will be a small fraction of the upper plenum radius in both prototype and model and so, perhaps, this will not be a significant distortion (the distortion will need to be further investigated both experimentally and analytically).

Scaling of eddy shedding frequency for cross-flow past posts may be important if either the prototype or model exhibit regular shedding frequencies. The prototype appears to have normal operation flow for much of the lower plenum in a Reynolds number (based on post diameter) range where eddy shedding for uniform flow across a cylinder is irregular ($3x10^5 < Re < 3x10^6$) (Huang and Lin, 2000). Reynolds numbers, based on post diameter, in the prototype range from approximately $5x10^4$ to 10^6. Eddy-shedding frequency f is characterized by non-dimensional Strouhal number St = f D/V. Frequency, in general, is not matched in a scaled system when Reynolds number is matched (since it depends on the product rather than the division of D and V). Flow visualization in the MIR experiments (using air bubbles) shows that no visually apparent frequency is associated with eddy shedding. This may be due to the wide range of (vector) velocities impinging on each of the cylinders. However, detailed velocity measurements and analyses of the MIR experiments may show a peaked frequency spectrum that is not apparent visually.

Table 1. Comparison of working fluids for VHTR scale models. VHTR natural circulation decay-heat conditions based on RELAP5/ATHENA calculations at 144,000 s after scram (Bayless, 2006).

Model	$\mathrm{Re}_m / \mathrm{Re}_p$ for lower plenum N.C. if $Ri_m = Ri_p$	Flow visualization, PIV and PLIF	Max. flow rate ($\mathrm{Re}_{\text{L.P. noz.}} = 7{,}000$)	**Significant problems**
Heavy-gas Injection (Ar)	0.16	Good in U.P. Mediocre in L.P.	315 CFM	Venting of Argon gas
Heavy-gas Injection (SFl6)	0.25	Good in U.P. Mediocre in L.P.	51.3 CFM	Venting or separating SFl6 from N2
Heated gas[1] (air)	0.079	Good in U.P. Mediocre in L.P.	315 CFM	Thermal stress Low Re Non-transparent components
Heated water[2]	1.0	Good in both L.P. and U.P.	200 GPM	Index-of-refraction variations
Water plus dissolved solid[3]	0.76	Good in both L.P. and U.P.	200 GPM	Disposal of large volumes of salt water

1. Assumes 20 ^{o}C cold gas and 80 ^{o}C hot gas.
2. Assumes 20 ^{o}C cold water and 46 ^{o}C hot water for simulated natural circulation flow and 20 ^{o}C and 30 ^{o}C for turbulent flow in lower plenum.
3. Assumes $(\Delta\rho / \rho)_{\mathrm{model}} = (\Delta\rho / \rho)_{prototype}$

Reynolds Number Independence

The modeling methods workshop conducted in conjunction with the ICONE conference in Miami, July, 2006, brought up the issue of scaling very high Reynolds number flows in the point design VHTR in a small-scale facility which will have, as a practical necessity, flows with lower Reynolds numbers. Although Reynolds numbers for natural circulation can be matched in the plenum experiments, forced circulation Reynolds numbers will be considerably lower. For example, for full-power operation the lower plenum nozzle Reynolds number will be approximately 200,000, while the maximum achievable model Reynolds number will be about 7,000 to 8,000.

The problem of modeling very high Reynolds number (turbulent and subsonic) flow in a small-scale facility at lower, but still turbulent, Reynolds number is a common situation in wind tunnel and other flow tunnel experiments. The usual argument is that if the flow is fully turbulent and if the phenomena in question vary only slowly with Reynolds number, and asymptotically approach an infinite Reynolds number value (the flow field of which, for incompressible flow, corresponds to potential flow outside of recirculation regions), then the experimental results are representative of the higher Reynolds number flow. Common examples include the velocity profile and wall friction factor for internal flow and the flow field and coefficients of drag and lift for flow over airplane wings and other components. Examples of comparisons of complex mixing flows in lower Reynolds number experiments with full-scale prototypes that are relevant for our plenum experiments include MacDonald et al., 1998 and Snyder, 1981. The guidelines that these two authors and others provide is that for flow over objects, such as the lower plenum posts, Reynolds numbers must be over a threshold value of 4,000 in order to provide large-scale flow similarity and Reynolds number independence. If nozzle Reynolds number is a minimum of 4,000 then jets entering the lower plenum will have a fully-turbulent profile, the jets within the plenum will be fully turbulent and flow across posts and in areas of the plenum away from posts will be fully turbulent and large and small eddy flow structures will be scaled. Reynolds number independence can be tested in experiments by varying the flow through the maximum achievable range for turbulent flow and comparing any differences, for example by varying lower-plenum Reynolds numbers for the larger nozzles from 3,000 to 7,000.

Instrumentation

The primary instrumentation for the experiments will consist of flow meters, thermocouples, pressure transducers, Particle Image Velocimeter (PIV), and Planar Laser Induced Fluorescence (PLIF). Flow meters will be employed to measure overall flow rate plus individual flow rates delivered to the nine manifolds that feed the individual tubes. Flows delivered to the individual tubes will be calibrated (and adjusted) as functions of manifold flow rates.

The primary measurements of velocities and velocity fluctuations will be performed using a LaVision 3D PIV that is presently being employed for the MIR experiments (McIlroy et al., 2006). The PIV system employs a laser light sheet for illumination. The vector velocity field is measured in the plane of the light sheet plus the velocity component transverse to the light sheet. The light sheet may be positioned between rows of tubes or along the center-lines of tubes, as shown in Figure 9, or perpendicular to and intersecting the tubes. Because the index-of-refractions of water and the (plastic or glass) tube material are not exactly matched, PIV may be restricted to the two-dimensions of the laser light sheet when the light sheet is parallel to the tubes. The restriction to two dimensions is due to the requirement of two cameras for the stereoscopic view required for 3D PIV and because the view is probably limited to one direction for this geometry. When the light sheet is perpendicular to the tubes and viewed from above or below the plenums, 3D PIV may be possible. The method of viewing between rows of tubes is to employ a cylindrical concave mirror as shown in Figure 9. Parallax divergence of view of the tube rows may be eliminated by placing the camera at the infinity focal position of the mirror. This method was used for flow visualization in experiments that simulated core flow and dye injection in a reactor core bundle (McCreery et al., 1990). The method was successfully employed to visualize flow and map dye concentration in the majority of the bundle cross-section, such as in the view shown in Figure 10.

Temperature distribution may be measured by the conventional method of using thermocouples, including using thermocouple rakes and thermocouples attached to traversing rods and by Planar Laser Induced Fluorescence (PLIF) (Nash et al., 1995). PLIF is an extension of PIV in that it uses the same laser and video recording devices. For PLIF, tracer particles will be used that fluoresce with an intensity that is a function of temperature. Two-dimensional temperature fields may thereby be measured and mapped.

Concluding Remarks

Various scaled heated gas and water flow facilities were investigated for modeling VHTR upper and lower plenum flows during the decay heat portion of a pressurized conduction-cooldown scenario and for modeling thermal mixing and stratification ("thermal striping") in the lower plenum during normal operation. It is concluded, based on phenomena scaling and instrumentation and other practical considerations, that a heated water flow scale model facility is preferable to a heated gas flow facility and to unheated facilities which use fluids with ranges of density to simulate the density effect of heating. For a heated water flow lower plenum model, both the Richardson numbers and Reynolds numbers may be approximately matched for conduction-cooldown natural circulation conditions. Thermal mixing during normal operation may be simulated but at lower, but still fully turbulent, Reynolds numbers than in the prototype. Natural circulation flows in the upper plenum may also be simulated in a separate heated water flow facility that uses the same plumbing as the lower plenum model. However, Reynolds number scaling distortions will occur at matching Richardson numbers due primarily to the necessity of using a reduced number of channels connected to the plenum than in the prototype (which has approximately 11,000 core channels connected to the upper plenum) in an

otherwise geometrically scaled model. These scaling distortions may be characterized by running series of experiments with varying flow rates and temperatures. Experiments conducted in either or both facilities will meet the objectives of providing benchmark data for the assessment and improvement of codes proposed for NGNP designs and safety studies, as well as providing a better understanding of the complex flow phenomena in the plenums.

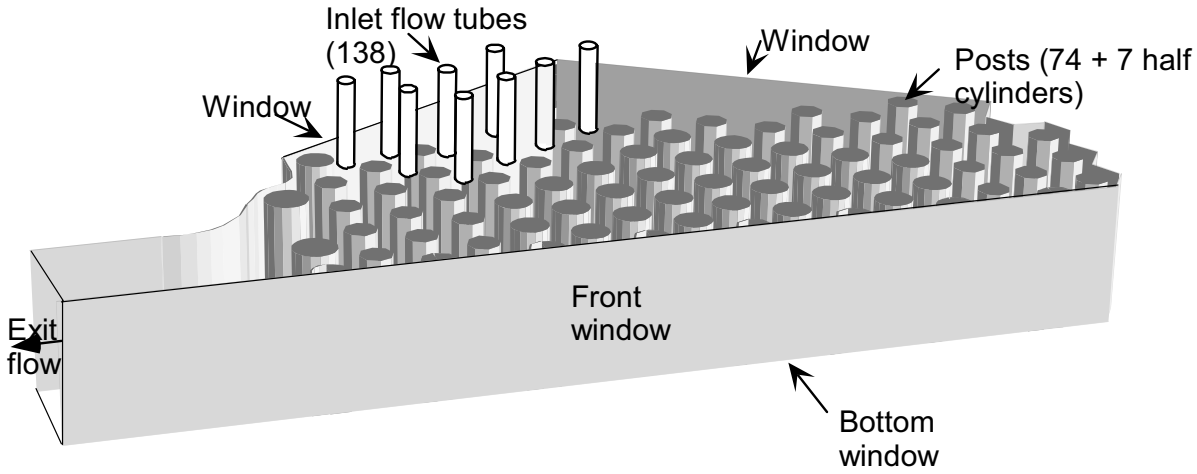

Figure 2. Isometric view of lower plenum model.

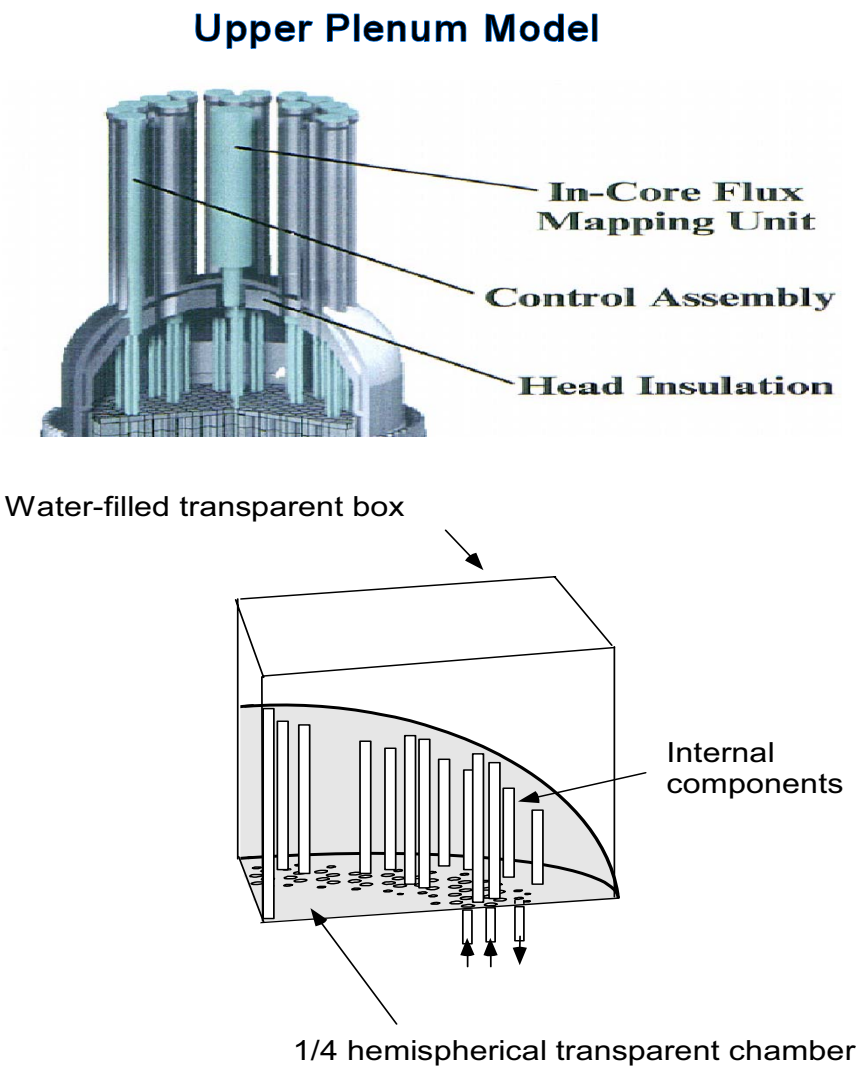

Figure 3. Upper plenum prototype and model

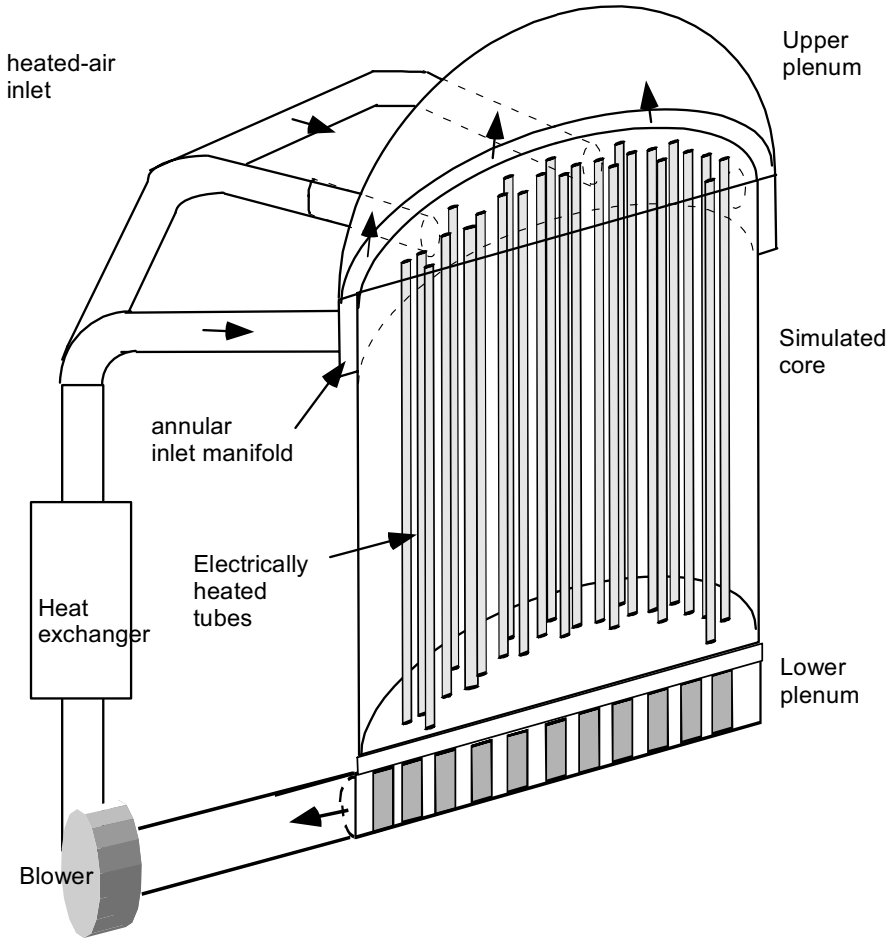

Figure 4. Geometrically scaled one-half symmetric model of VHTR vessel employing gas flow and an electrically-heated core.

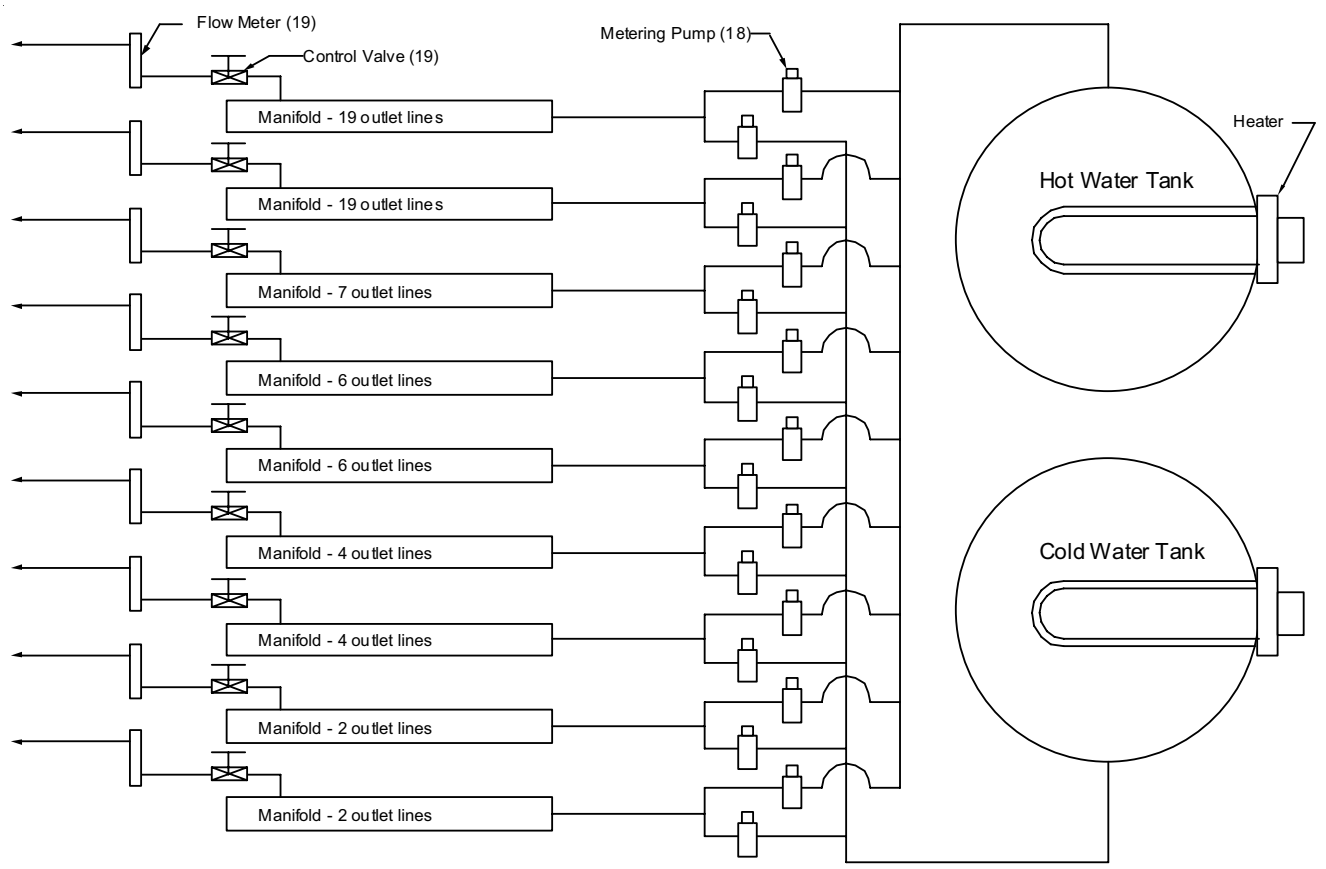

Figure 5. Plumbing schematic. Water flow rates and temperatures delivered to each of the nine manifolds are controlled by metering flows from the hot and cold water storage tanks. Individual lines (with valves) connect the manifolds to the nozzles.

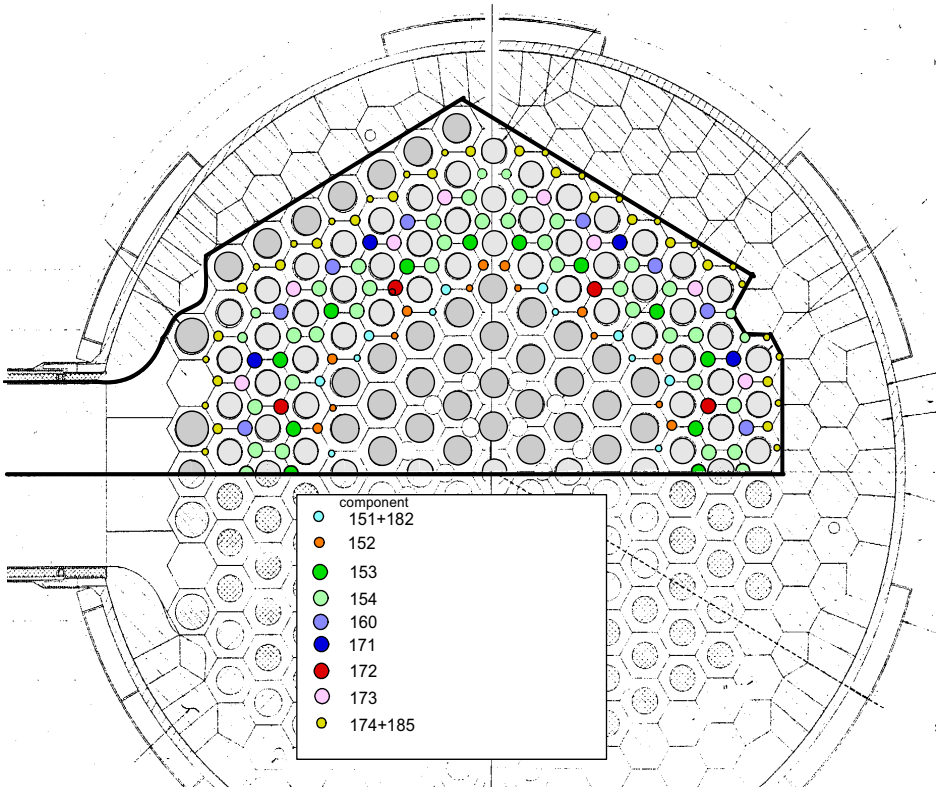

Figure 6. Nine region flow map of lower plenum and corresponding RELAP5/ATHENA model components.

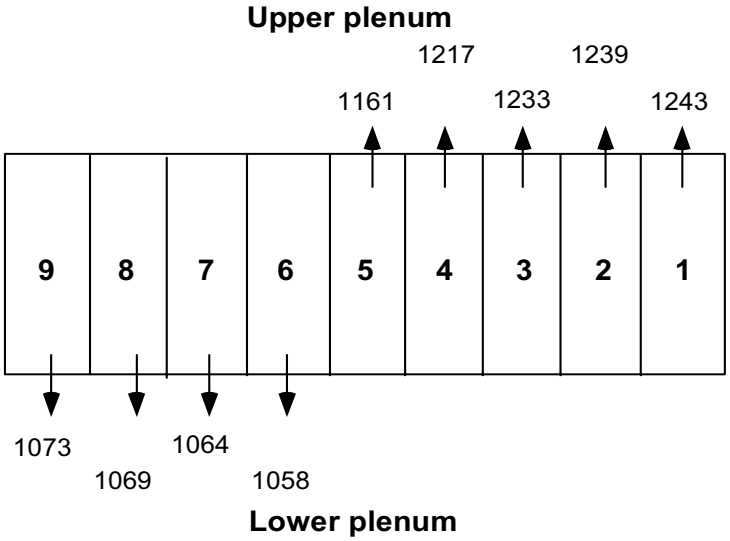

Plenum entrance (core exit) temperatures (K) in prototype at 144,000 s following scram for conduction-cooldown.

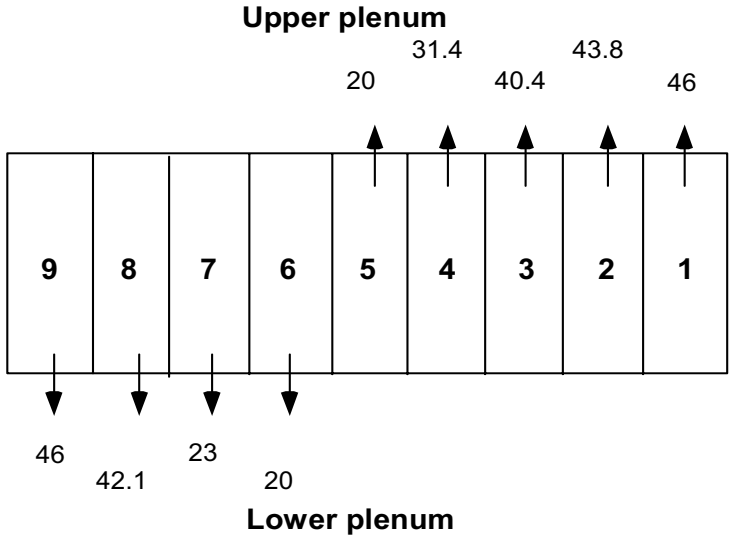

Scaled model plenum entrance temperatures (K).

Figure 7. Plenum entrance temperatures in prototype predicted by RELAP5/ATHENA calculations and corresponding scaled model temperatures (^{o}C).

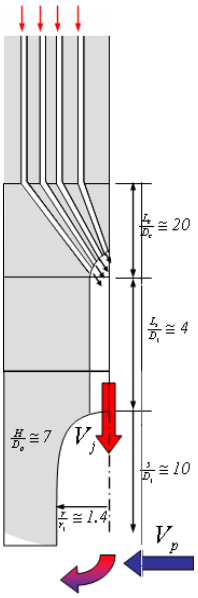

Figure 8. Geometry of core channels merging into a lower plenum nozzle.

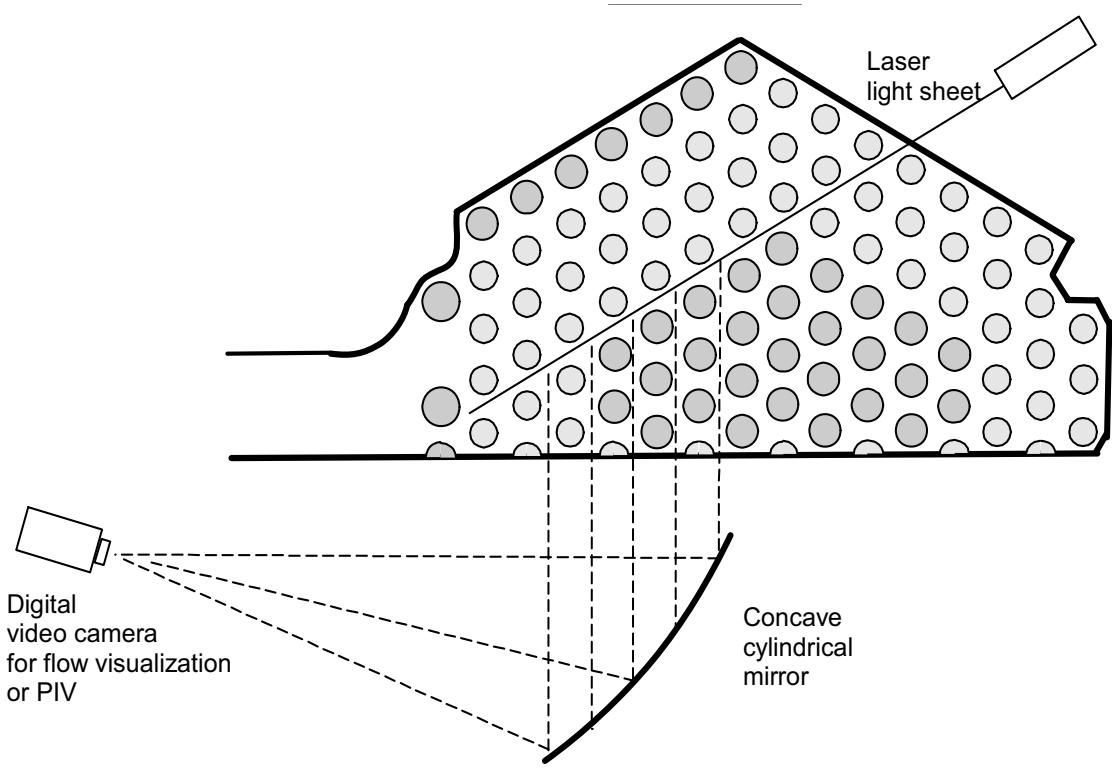

Figure 9. PIV and PLIF optical instrumentation set-up for lower plenum.

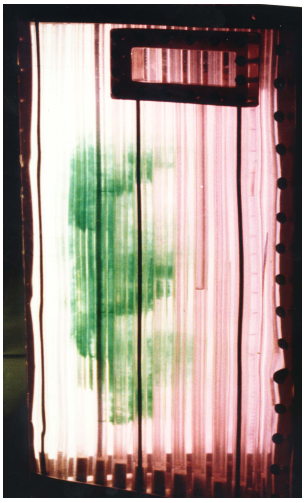

Figure 10. Dye injection in 1/6 sector model core with water flow. The dye plume is mostly visible between and through water-filled tubes.

References:

Bayless, P.D., 2006, "RELAP5/ATHENA calculations of VHTR conduction-cooldown", private communication.

Huang, R.F., and Lin, C.L., 2000, "Velocity field of a bluff body wake", J. Wind Engineering and Industrial Aerodynamics 85 , p. 31-45.

Inagaki, Y, Kunugi, T., and Miyamoto, Y., 1990, "Thermal mixing test of coolant in the core bottom structure of a high temperature engineering test reactor", Nuc. Engr. And Design, 123, pp. 77-86.

Inagaki, Y, Kunitomi, K., Miyamoto, Y, Ioka, I., and Suzuki, K., 1992, "Thermal-hydraulic characteristics of coolant in the core bottom structure of the high-temperature engineering test reactor",Nuclear Technology, vol. 99, pp. 90-102.

King, J.B., 2004, "Mixing in the VHTR lower-plenum: decomposition, data, and analysis", Technical Report (Draft), Department of Nuclear Engineering, Oregon State University.

MacDonald, R., Griffiths, R., and Hall, D., 1998, "A comparison of results from scaled field and wind tunnel modeling of dispersion in arrays of obstacles", Atmos. Environment, 32, pp. 3845-3862.

P. E. MacDonald, J. W. Sterbentz, R. L. Sant, P. D. Bayless, R. R. Schultz, H. D. Gougar, R. L. Moore, A. M. Ougouag, and W. K. Terry, 2003 "NGNP Preliminary Point Design – Results of the Initial Neutronics and Thermal-Hydraulic Assessments," Tech. Rpt. INEEL/EXT-03-00870 Rev. 1.

McCreery, G.E., Stoots, C.M., and Boucher, T.J., 1991, "Scaled Experiments for the Study of Nuclear Reactor Upper Plenum Flow Phenomena", Proceedings *ASME/AIChE/ANS Natl. Heat Transfer Conf.*, Minneapolis.

McCreery, G.E., McKellar, M.G., and Stoots, C.M., 1990, "Steady-state and transient moderator flow and ink dispersion tests", EGG-EAST-9382.

McEligot, D.M., and McCreery, G.E., "Initial scaling studies and conceptual thermal fluids experiments for the prismatic NGNP point design", INEEL/EXT-04-02367, Sept. 30, 2004.

McIlroy, H.M., McEligot, D.M., McCreery, G.E., Condie, K.G., and Pink, R.J., "Experimental Measurement of Flow Phenomena in a VHTR Lower Plenum Model", ANS Annual Meeting, Reno, NV, June, 2006.

Nash, J.D., Jirka, H., and Chen, D., 1995, “Large scale planar laser induced fluorescence in turbulent density-stratified flows”, Exp. In Fluids, 19, pp. 297-304.

Snyder, W.H., 1992, “Guidelines for fluid modeling of atmospheric dispersion”, Report EPA-600/8-81-009, Research Triangle Park, N.C.

Tauveron, N., 2002, “Thermal fluctuations in the lower plenum of a high temperature reactor”, Nuclear Engineering and Design, 222, pp. 125-137.

Triton, D.J., 1977, “Physical Fluid Dynamics”, Van Nostrand Reinhold, New York.

Turner, J.S., 1973, “Buoyancy Effects in Fluids”, Cambridge University Press, London.

Westinghouse Electric Corporation, 1990, “Experiments on natural circulation during PWR severe accidents”, Internal Report. See also, EPRI NP-6324-D, July, 1989.

Appendix A. Jet entrainment scaling

Since jet entrainment of ambient fluid is identified in preliminary flow visualization experiments and in the literature as being of prime importance to scaling, it is investigated in more detail.

Consider a geometrically scaled model with length ratio L = prototype length/model model length

Model lengths,
Z' = Z/L
Y' = Y/L
X' = X/L

Volume
$V' = V/L^3$
Area
$A' = A/L^2$

Consider a jet with flow rate Q_j and velocity V injected into cross-flow with velocity V_{cf} Assume that $V >> V_{cf}$, which is the case for lower plenum flow except near the exit. (Schetz, 1980, addresses the more general case in which the equations are the same except that V is replaced by $V-V_{cf}$).

For turbulent forced jets, List (1982) and Peterson (1994) provide an empirical relationship for jet volumetric entrainment rate, Q_e,

$$\frac{dQ_e}{dZ} = \alpha_T \sqrt{8\pi M} \qquad \text{(A1)}$$

where

α_T = Taylor jet entrainment constant

M = jet momentum = $4Q_0^2 / \pi d^2$

Q_0 = jet flow rate

d = jet orifice diameter

It is assumed that, for a forced jet, momentum flux is conserved along the path of the jet. This assumption leads to the conclusion that a turbulent jet has a constant aspect ratio with Z (spreads with a constant angle) that is independent of Reynolds number, which is approximately true according to List (1982) and Peterson (1994).

Rearranging equation A1,

$$\frac{dQ_e}{dZ} = \alpha_T \sqrt{8\pi} \frac{2Q_0^2}{\pi d}$$

If volumetric flow rate in the model (Q') is scaled such that

$Q' = Q/L^n$

Then the non-dimensional entrainment rate is scaled as,

$$\frac{dQ'_e}{dZ'} = \alpha_T \sqrt{8\pi} \frac{2Q'_0}{\pi d'}$$

Velocity is scaled as,

$V' = V/L^{n-2}$

and Reynolds number,

$$\mathrm{Re}' = V'Z'/\nu' = \frac{\mathrm{Re}}{L^{n-1}(c\nu)}$$

Where, kinematic viscosity, $\nu' = c\nu$.

If, for the simulated thermal experiment, water at approximately ambient temperature is used as a substitute for helium at operating conditions, then,
$c \approx 1/5$

and,

$$\mathrm{Re}' \approx \frac{5}{L^{n-1}\nu}$$

Non-dimensional entrainment is therefore approximately independent of Reynolds number in a geometrically scaled system. If for example, L = 6.55 for our chosen model scale, then if c= 1/5 and n = 2 then Re' = Re and V' = $\frac{Q}{AL^{n-2}} = V$
V'=V is unreasonably large (approximately 32 m/s for the NGNP) for a model water flow system so Re' will be less than Re for reasonable velocities.

Jet Reynolds number should be sufficiently large that turbulent jets are insured (Rejet > a few 10's, according to Triton, 1977), which sets a minimum scaling factor for V'.

Since jet divergence angle is approximately constant for a turbulent jet as a function of Reynolds number (Peterson, 1994), the geometry of interactions should be approximately scaled in a geometrically scaled model. The Coanda effect will, however, increase the divergence angle between closely spaced jets and draw jets to nearby walls; which is observed in the MIR experiments. The Coanda effect is caused by jet fluid entrainment. If jet entrainment is well scaled, then jet divergence angles should also be well scaled.

Appendix A1 references:

Dimotakis, P.E., Miake-Lye, R.C., Papantoniou, D.A., 1983, "Structure and dynamics of round turbulent jets", Phys. Fluids, 26 (11), pp. 3185-3192.

Guo, B., Langrish, T.A.G., and Fletcher, D.F., 2001, "An assessment of turbulence models applied to the simulation of a two-dimensional submerged jet", Applied mathematical modeling, 25, pp. 635-653.

Kelso, R.M., Lim, T.T., and Perry, A.E., 1996, "An experimental study of round jets in cross-flow", J. Fluid Mech., vol. 306, pp. 111-144.

Nobes, J.M., and Nathan, G.J., 2001, "Influence of jet exit conditions on the passive scalar field of an axisymmetric free jet", J. Fluid Mech., vol. 432, pp. 91-125.

Peterson, P.F.,1994, "Scaling and analysis of mixing in large stratified volumes", Int. J. Heat Mass Transfer, vol. 37, pp. 97-106.

Smith, S.H., and Mungal, M.G., 1998, "Mixing, structure and scaling of the jet in crossflow", J. Fluid Mech., vol 357, pp. 83-122.

Rodi, W., 1982, "turbulent buoyant jets and plumes", Pergammon Press, New York.

Schetz, J.A., 1980, "Injection and mixing in turbulent flow", vol. 68, Progress in Astronautics and aeronautics, Summerfeld, M., Editor, AIAA.

Triton, D.J., 1977, "Physical Fluid Dynamics", Von Nostrand, New York.

Appendix B. Preliminary design drawings.

A series of dimensioned drawings were generated that serve both as illustrations of the basic design concepts and the foundation of the detailed model design. The drawings were generated using VectorWorks, a 2D/3D computer aided drafting and design program developed by Nemetschek North America. Objects can be drawn in 2D and extruded into 3D or drawn directly in 3D. Multiple layers of objects can be linked together to generate complex 3 dimensional illustrations while retaining the details of each object to be used for manufacturing of individual piece parts.

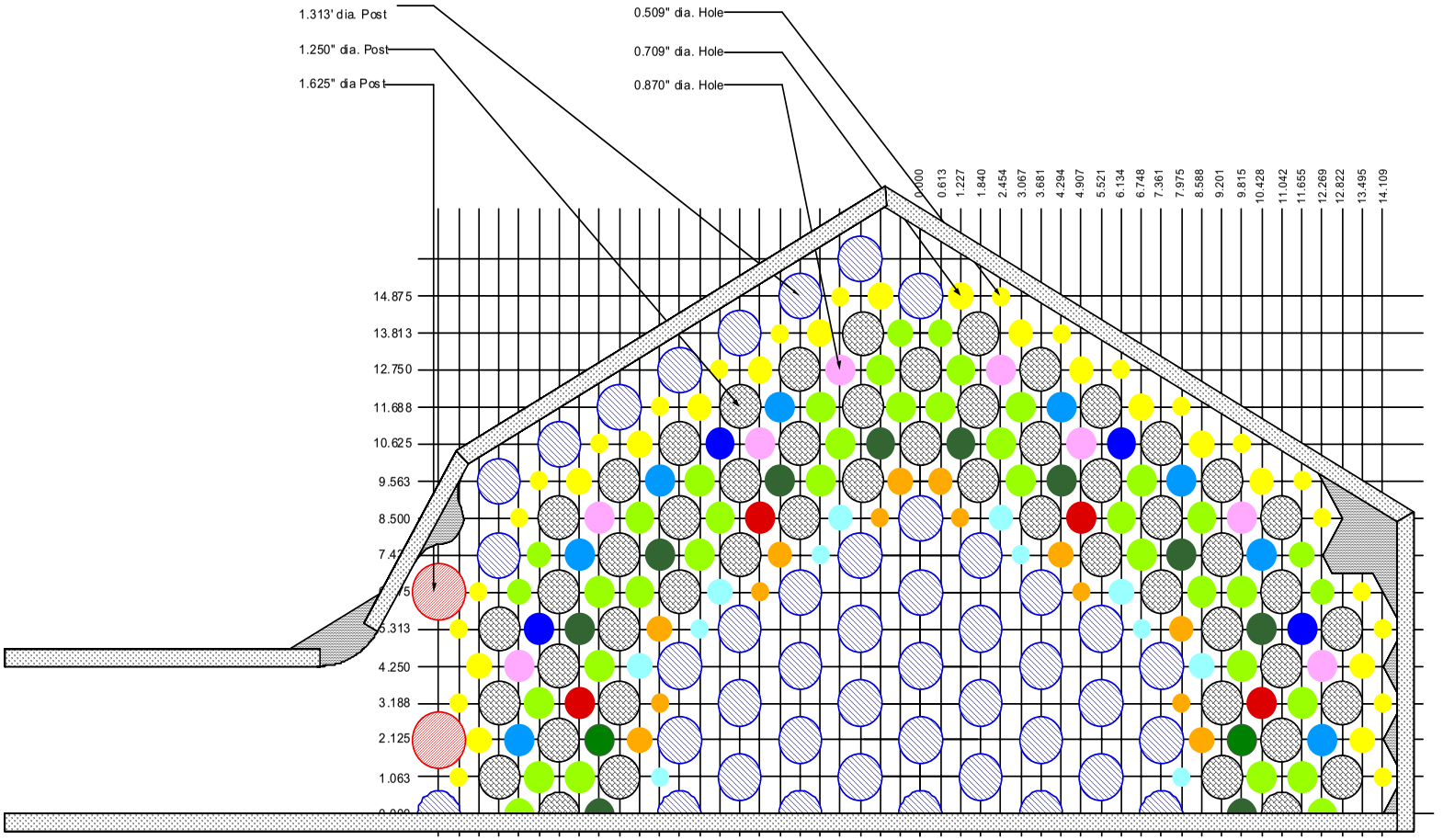

Figure B1. Top view of lower plenum showing (with dimensions in inches) posts, nozzles, walls, filler-pieces and windows.

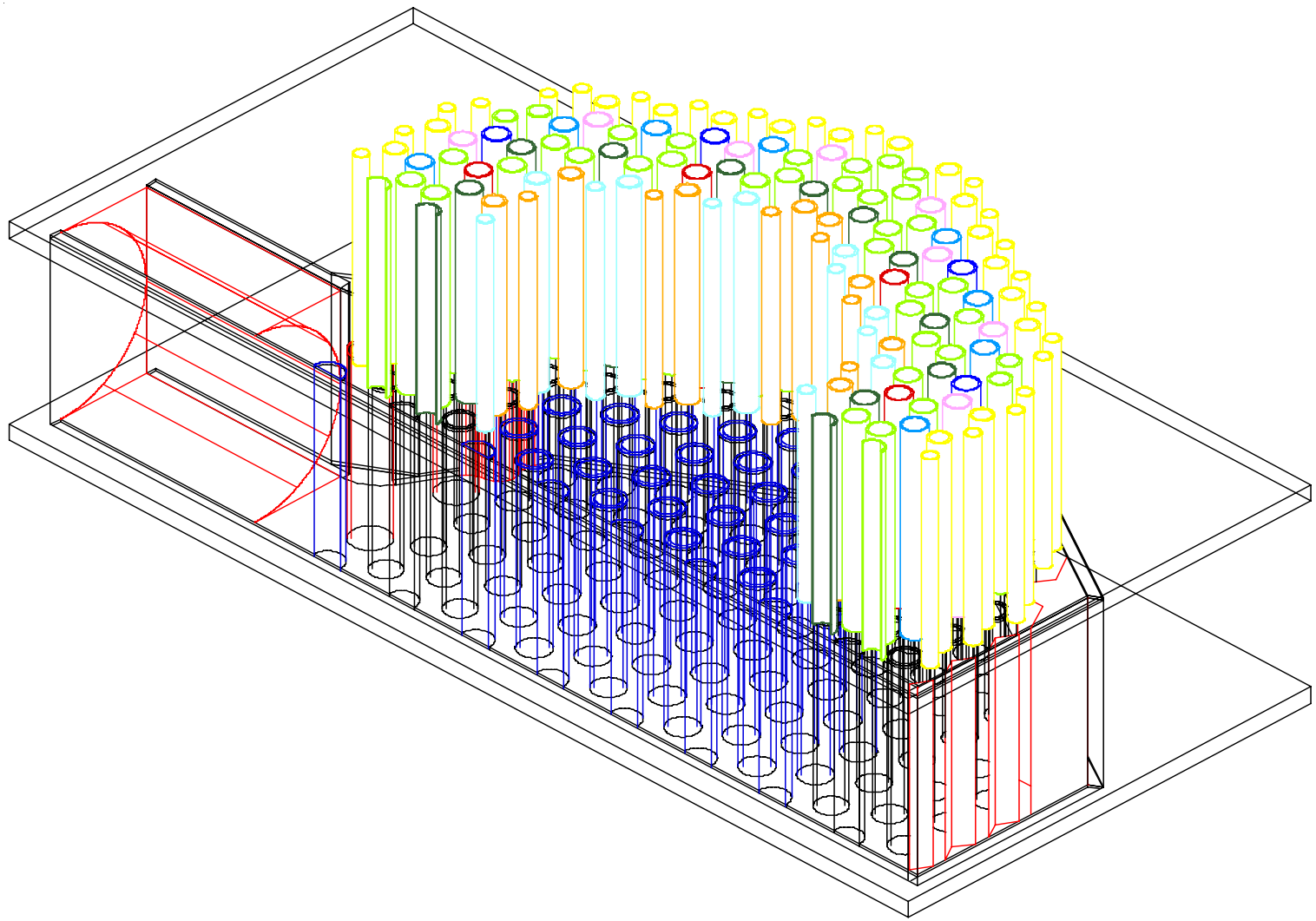

Figure B2. Three-dimensional view of lower plenum model showing construction details including posts, outlet nozzle, top and bottom sheets and inlet tubes.

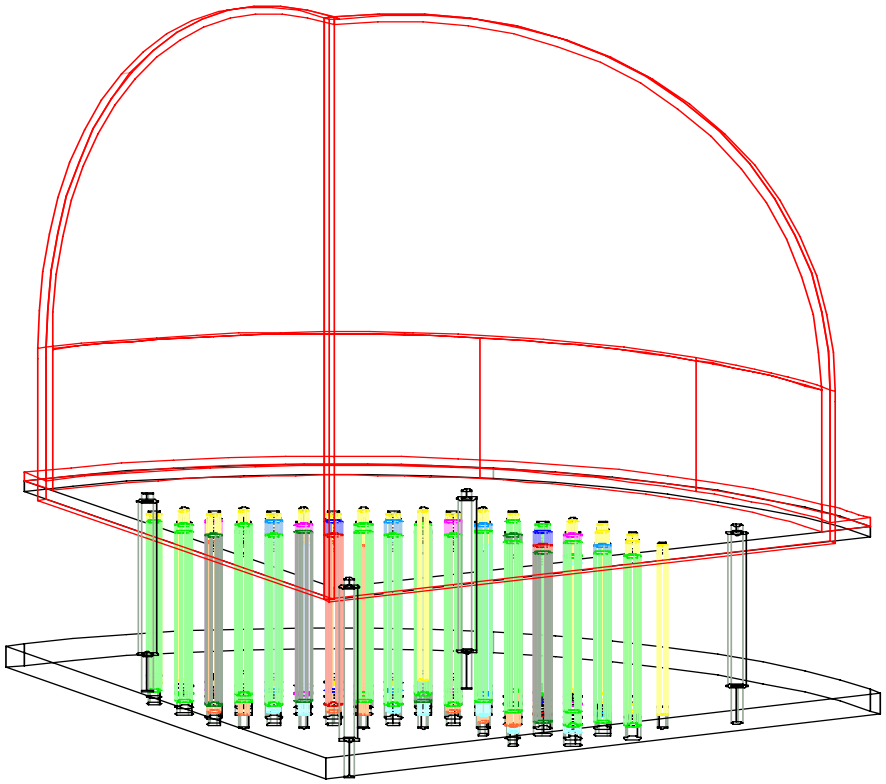

Figure B3. Upper plenum model without internal components or rectangular box enclosure. Inlet tubes are shown.